



















# Differences in atrial substrate localization using late gadolinium enhancement-magnetic resonance imaging, electrogram voltage, and conduction velocity: a cohort study using a consistent anatomical reference frame in patients with persistent atrial fibrillation

Deborah Nairn <sup>1†</sup>, Martin Eichenlaub <sup>2,3†</sup>, Björn Müller-Edenborn <sup>2,3</sup>,  
Taiyuan Huang <sup>2,3</sup>, Heiko Lehrmann <sup>2,3</sup>, Claudia Nagel <sup>1</sup>, Luca Azzolin <sup>1</sup>,  
Giorgio Luongo <sup>1</sup>, Rosa M. Figueras Ventura <sup>4</sup>, Barbara Rubio Forcada <sup>4</sup>,  
Anna Vallès Colomer <sup>4</sup>, Dirk Westermann <sup>2,3</sup>, Thomas Arentz <sup>2,3</sup>,  
Olaf Dössel <sup>1</sup>, Axel Loewe <sup>1\*‡</sup>, and Amir Jadidi <sup>2,3,5‡</sup>

<sup>1</sup>Institute of Biomedical Engineering, Karlsruhe Institute of Technology (KIT), Fritz-Haber-Weg 1, Karlsruhe 76131, Germany; <sup>2</sup>Department of Cardiology and Angiology, Medical Center, University of Freiburg, Freiburg, Germany; <sup>3</sup>Faculty of Medicine, University of Freiburg, Freiburg, Germany; <sup>4</sup>Adas 3D Medical SL, Carrer Paris 179, Barcelona, Spain; and <sup>5</sup>Arrhythmia Division, Department of Cardiology, Heart Center Lucerne, Lucerne Cantonal Hospital, Lucerne, Switzerland

Received 12 June 2023; accepted after revision 10 September 2023; online publish-ahead-of-print 15 September 2023

## Aims

Electro-anatomical voltage, conduction velocity (CV) mapping, and late gadolinium enhancement (LGE) magnetic resonance imaging (MRI) have been correlated with atrial cardiomyopathy (ACM). However, the comparability between these modalities remains unclear. This study aims to (i) compare pathological substrate extent and location between current modalities, (ii) establish spatial histograms in a cohort, (iii) develop a new estimated optimized image intensity threshold (EOIIT) for LGE-MRI identifying patients with ACM, (iv) predict rhythm outcome after pulmonary vein isolation (PVI) for persistent atrial fibrillation (AF).

## Methods and results

Thirty-six ablation-naïve persistent AF patients underwent LGE-MRI and high-definition electro-anatomical mapping in sinus rhythm. Late gadolinium enhancement areas were classified using the UTAH, image intensity ratio (IIR >1.20), and new EOIIT method for comparison to low-voltage substrate (LVS) and slow conduction areas <0.2 m/s. Receiver operating characteristic analysis was used to determine LGE thresholds optimally matching LVS. Atrial cardiomyopathy was defined as LVS extent ≥5% of the left atrium (LA) surface at <0.5 mV. The degree and distribution of detected pathological substrate (percentage of individual LA surface area) varied significantly ( $P < 0.001$ ) across the mapping modalities: 10% (interquartile range 0–14%) of the LA displayed LVS <0.5 mV vs. 7% (0–12%) slow conduction areas <0.2 m/s vs. 15% (8–23%) LGE with the UTAH method vs. 13% (2–23%) using IIR >1.20, with most discrepancies on the posterior LA. Optimized image intensity thresholds and each patient's mean blood pool intensity correlated linearly ( $R^2 = 0.89$ ,  $P < 0.001$ ). Concordance between LGE-MRI-based and LVS-based ACM diagnosis improved with the novel EOIIT applied at the anterior LA [83% sensitivity, 79% specificity, area under the curve (AUC): 0.89] in comparison to the UTAH method (67% sensitivity, 75% specificity, AUC: 0.81) and IIR >1.20 (75% sensitivity, 62% specificity, AUC: 0.67).

\* Corresponding author. Tel: +49-721-608-42790, E-mail address: publications@ibt.kit.edu

† The first two authors contributed equally to the study.

‡ The last two authors contributed equally to the study.

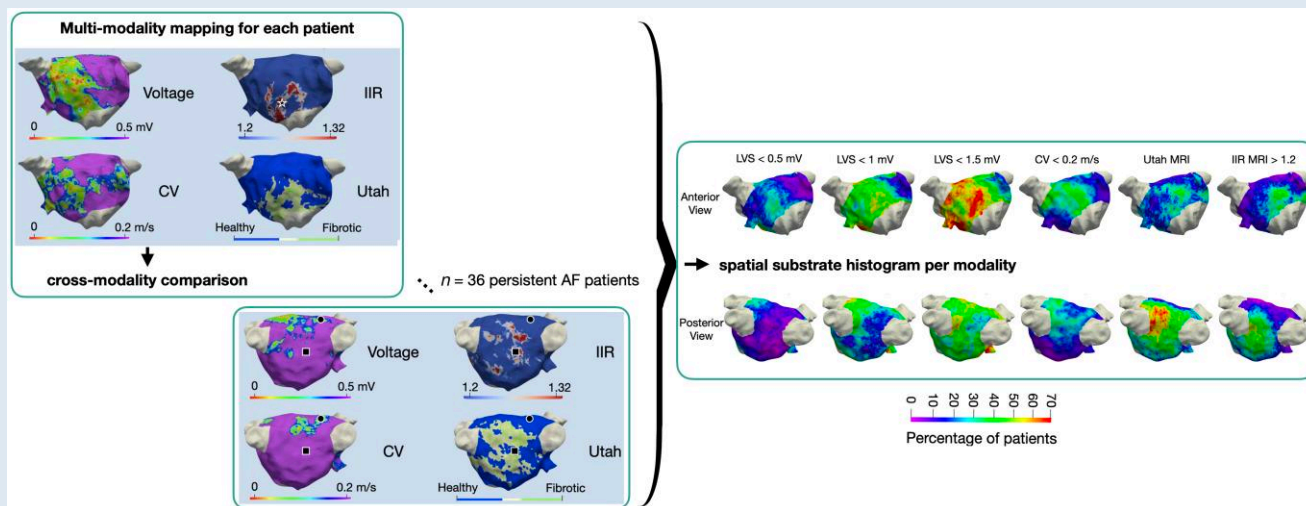
© The Author(s) 2023. Published by Oxford University Press on behalf of the European Society of Cardiology.

This is an Open Access article distributed under the terms of the Creative Commons Attribution-NonCommercial License (<https://creativecommons.org/licenses/by-nc/4.0/>), which permits non-commercial re-use, distribution, and reproduction in any medium, provided the original work is properly cited. For commercial re-use, please contact journals.permissions@oup.com

## Conclusion

Discordances in detected pathological substrate exist between LVS, CV, and LGE-MRI in the LA, irrespective of the LGE detection method. The new EOIIT method improves concordance of LGE-MRI-based ACM diagnosis with LVS in ablation-naïve AF patients but discrepancy remains particularly on the posterior wall. All methods may enable the prediction of rhythm outcomes after PVI in patients with persistent AF.

## Graphical Abstract



## Keywords

Atrial fibrillation • LGE-MRI • Electro-anatomical mapping • Conduction velocity • Atrial cardiomyopathy

## What's new?

- Voltage mapping, late gadolinium enhancement (LGE) magnetic resonance imaging (MRI) and conduction velocity mapping identify different atrial cardiomyopathy (ACM) areas, particularly on the posterior wall of the left atrium.
- First side-by-side statistical atlas of all three substrate mapping modalities.
- A new LGE-MRI post-processing method (estimated optimized image intensity threshold at the anterior wall) increasing concordance with voltage mapping for the diagnosis of ACM.
- Estimated optimized image intensity threshold at the anterior wall may be suitable for prediction of rhythm outcome after pulmonary vein isolation.

## Introduction

Atrial fibrillation (AF) is the most common cardiac arrhythmia causing an irregular heart rhythm, is associated with an increased risk for stroke and heart failure.<sup>1</sup> Pulmonary vein isolation (PVI) is a common treatment for AF with a high success rate (75–90%) in paroxysmal AF patients.<sup>2</sup> However, persistent AF patients may present atrial cardiomyopathy (ACM) with extra-pulmonary vein (PV) pathological substrate, which contributes to the maintenance of AF and reduces the success rate markedly.<sup>3,4</sup> A lack of consensus and standardization on how to locate ACM substrate may be part of the reason for suboptimal treatment success in persistent AF patients.<sup>3,5–7</sup>

Electro-anatomical mapping (EAM) during sinus rhythm (SR) identifying low-voltage bipolar electrograms (<0.5 mV) is a common

technique used to locate pathological substrate.<sup>8,9</sup> Voltage-guided ablation has recently been shown to improve SR maintenance in a randomized controlled trial (RCT).<sup>10</sup> Conduction velocity (CV) mapping has also been investigated due to the structural and functional abnormalities resulting in conduction slowing.<sup>11–14</sup> Another commonly used method is late gadolinium enhancement (LGE) magnetic resonance imaging (MRI).<sup>15–17</sup> The advantage of LGE-MRI is that it is a less invasive diagnostic method. However, the spatial resolution of LGE-MRI is limited. Although all the above-mentioned methods detect pathological substrates, discordances in their location and extent have been reported.<sup>18,19</sup> Furthermore, different post-processing methods may contribute to LGE-MRI discrepancies.<sup>19,20</sup> In contrast to EAM, LGE-MRI-guided ablation has not been able to improve SR outcome after ablation in the recently published DECAAF II RCT.<sup>5</sup>

In this study, we systematically compare the spatial distribution of pathological left atrial (LA) substrate as detected in LGE-MRI (using various MRI post-processing methods), voltage, and CV mapping during SR in ablation-naïve AF patients on a point-by-point basis. Spatial histograms of substrate frequency in each modality are established using a statistical shape model. Additionally, a new estimated optimized image intensity thresholding (EOIIT) method for LGE-MRI is proposed to enable more accurate identification of patients with ACM as diagnosed by low-voltage areas <0.5 mV in SR.

## Methods

### Patient sample

Forty-one consecutive patients undergoing first PVI for symptomatic persistent AF (lasting >7 days and <12 months) who met the indication criteria according to European guidelines<sup>1</sup> were included prospectively at the

University Heart Center Freiburg Bad Krozingen between February 2019 and July 2019 (DRKS00014687). Patient characteristics are detailed in *Table 1*. All patients were electrically cardioverted into SR 4–6 weeks before PVI. Patients with AF recurrence on readmission for PVI underwent repeat electrical cardioversion 1 day before the PVI procedure. One patient with AF refractory to electrical cardioversion, two patients with incomplete MRI (one due to claustrophobia, one due to bradycardia during MRI), one patient due to insufficient MRI image quality, and one patient due to technical issues during analysis had to be excluded. The study was approved by the institutional ethics committee and all patients provided written informed consent before enrolment.

## Electro-anatomical mapping

High-density (>1200 mapped sites per LA) activation and voltage mapping were performed using a 20-polar Lasso-Nav mapping catheter or a PentaRay catheter (electrode size: 1 mm, spacing: 2–6 mm). Mapping was conducted while the patient was in SR before PVI using the CARTO-3 mapping system (Biosense Webster, Diamond Bar, CA, USA). All areas demonstrating low voltage in the multi-electrode mapping catheter were confirmed using a separate contact force sensing mapping catheter with a contact threshold of >5 g. Further details about the signal processing and calculation of the local activation time (LAT), voltage, and CV are given in the [Supplementary material online, Section S1.1](#). The study was approved by the institutional ethics committee of the University of Freiburg (Germany) and all patients provided written informed consent before enrolment.

In three series of analyses, cut-off values of <0.5, <1.0, and <1.5 mV were applied to the bipolar voltage maps to define the low-voltage substrate (LVS).<sup>21,22</sup> For CV, the cut-off value for pathological slow-conducting substrate was set at 0.2 m/s.<sup>23</sup>

## Late gadolinium enhancement magnetic resonance imaging

Late gadolinium enhancement magnetic resonance imaging was performed on a 3T scanner (Somatom Skyra, Siemens Healthcare, Erlangen, Germany) as described previously.<sup>15,16</sup> In brief, LGE-MRI was acquired in SR 15 min after contrast injection with a dose of 0.1 mmol Gadoteridol per kg body weight (ProHance<sup>®</sup>, Bracco, Milan, Italy). Voxel size was 1.25 × 1.25 ×

2.5 mm (reconstructed to 0.625 × 0.625 × 1.25 mm), repetition time was 3.1 ms, echo time was 1.4 ms, and flip angle was 14°.

Two independent expert core laboratories performed the LA segmentation and detection of LGE areas: Merisight (Marrek Inc., Sandy, UT, USA) for the UTAH method and the Adas group (Adas3D Medical SL, Barcelona, Spain) for the image intensity ratio (IIR) method proposed by Benito *et al.*<sup>17</sup> All image analysts were blinded to any clinical characteristics. The LGE-MRI data of all patients were analysed using both methods with the output being annotated maps. Further details about the two methods can be found in the [Supplementary material online, Section S1.2](#).

## Follow-up

Ambulatory clinical visits including 12-lead-electrocardiogram (ECG) and 72 h Holter-ECG were scheduled 6 and 12 months after PVI. Arrhythmia recurrence was defined as any documented episode of AF, atypical atrial flutter, or atrial tachycardia lasting >30 s after a 3-month blanking period. If arrhythmia recurrence could not be detected by 12-lead-ECG and Holter-ECG, a single lead-ECG was registered by an event recorder any time patients suffered from symptomatic episodes.

## Analysis

### Left atrial mean geometry

Geometries obtained from each modality for all patients were aligned to a mean LA shape. Thus, a direct comparison between EAM and LGE-MRI and between patients could be performed without variations caused by spatial displacement as shown in previous studies.<sup>20,24,25</sup> The steps behind this approach are detailed in the [Supplementary material online, Section S1.2](#) and *Figure S1*. The PVs and mitral valve were excluded from all substrate analyses (see *Figure 2*). Conduction velocity estimation from the measured LAT map was done before mapping to the shape model instance.

## Statistical analysis

The median value for each point on the matched geometry across all patients was calculated for the voltage, CV, and LGE-MRI maps (image intensity values), providing a visual comparison between mapping modalities without the influence of outliers due to patient-specific differences.

A spatial histogram for each mapping modality was created to assess which areas most commonly exhibit pathological substrate. This provides for the first time a spatial histogram of LVS and slow conduction areas and a comparison of LGE-MRI spatial histograms with the one previously reported by Higuchi *et al.*<sup>26</sup>

Additionally, a correlation analysis was performed between each pair of mapping modalities identifying the difference in pathological substrate extent for each patient. All analyses were performed using MATLAB (version 2021b, The MathWorks, Natick, MA, USA).

### Detection of left atrial late gadolinium enhancement areas based on estimated optimized image intensity threshold 'EOIIT'

The individual patient's 'optimized image intensity threshold' (OIIT) with respect to the mean blood pool value of the LA LGE-MRI was identified as the threshold with a best quantitative match between LGE extent and LVS extent (<0.5 mV) and determined for each patient. *Figure 6* illustrates this concept. However, as the OIIT can only be determined if both LGE-MRI and voltage map are available for a given patient, the OIIT needs to be estimated if only LGE-MRI is available. Thus, a linear correlation was calculated for the entire cohort using a leave-one-out cross-validation method to determine the EOIIT (*Figure 6*). Three EOIIT values were determined for (i) the entire LA, (ii) the anterior LA, and (iii) the posterior LA. Details on the semi-automatic segmentation approach separating these three regions are given in the [Supplementary material online, Section S1.3](#) and *Figure S2*.

The performance of the new thresholds was then evaluated by examining the relationship between the LVS extent (<0.5 mV in SR) and LGE-MRI substrate for each LGE-MRI post-processing method (UTAH, IIR >1.20 and EOIIT).

Patients with an LVS extent of ≥5% of LA surface at <0.5 mV were classified as having substantial LVS.<sup>27</sup> Receiver operating curve analysis for substantial LVS was performed for the IIR >1.2 method and the EOIIT method for (i) the entire LA, (ii) the anterior LA and (iii) the posterior LA.

**Table 1** Patient clinical demographics

Patient characteristics	Total = 36
Age (years)	66 ± 9
Male (%)	31 (84)
BMI (kg/m <sup>2</sup> )	27.4 ± 3.5
LVEF (%)	57 ± 8
LA diameter (AP, mm)	47 ± 6
CHA <sub>2</sub> DS <sub>2</sub> -VASc score	2 (1–3)
Hypertension (%)	27 (73)
Diabetes mellitus (%)	3 (8)
Prior stroke or TIA (%)	1 (3)
Coronary artery disease (%)	5 (14)
Procedure duration (min)	146 ± 19
Successful circumferential PVI (%)	36 (100)
CTI ablations (%)	8 (22)
Prior antiarrhythmic therapy (%)	29 (78)

AP, anterior–posterior; BMI, body mass index; CTI, cavotricuspid isthmus; LA, left atrial; LVEF, left ventricular ejection fraction; PVI, pulmonary vein isolation; TIA, transient ischaemic attack.

## Results

### Patient characteristics

Thirty-six patients ( $66 \pm 9$  years old, 84% male) with persistent AF underwent LGE-MRI and EAM before PVI. All patients were electrically cardioverted 4–6 weeks before PVI. Fourteen patients (39%) with AF recurrence were cardioverted again on admission. *Table 1* provides details of the patient characteristics, procedural details for EAM and LGE-MRI data can be found in the supplementary material (see [Supplementary material online, Table S1](#)).

### Spatial distribution of left atrial pathological substrate in electro-anatomical voltage-activation mapping vs. late gadolinium enhancement

*Figure 1* reveals discrepancies in the distribution and extent of pathological substrate between EAM modalities and LGE-MRI. Both LGE-MRI methods identified extensive pathological substrate on the postero-inferior wall, whereas the electrograms in this area (marked with a square) are non-fractionated signals with high amplitudes. In contrast, low amplitude signals are seen (marked with a circle) where LVS and slow CV were identified. The locations marked with a star and a diamond show concordant substrate

assessment (enhancement and low voltage; no enhancement and normal voltage, respectively). The patient-specific substrate maps of each individual patient are shown in the [Supplementary material online, Figure S2](#).

On a population level, *Figure 2* reveals notable differences in the median voltages between the anterior [median 1.22 mV, interquartile range (IQR) 1.05–1.46 mV] and posterior wall (median 1.58 mV, IQR 1.34–1.90 mV). The CV shows similar differences although less pronounced (anterior: median 0.27 m/s, IQR 0.25–0.29 m/s and posterior: median 0.33 m/s, IQR 0.31–0.35 m/s). On the other hand, the LGE-MRI IIR method reveals relatively little difference between the anterior and posterior wall, with median IIR values of 0.98 (IQR 0.96–1.11) and 0.99 (IQR 0.90–1.12), respectively. Due to its discrete nature, the median for the UTAH method indicates 'fibrotic' wherever >50% of the patients exhibited enhancement (compare *Figure 3*). [Supplementary material online, Figures S5 and S6](#) separate the LGE-MRI vs. LVS analysis between the anterior wall and the rest of the LA; *S7* shows the correlations between all modalities and corresponding Bland–Altman plots.

### Spatial localization frequency of atrial sites displaying pathological substrate

*Figure 3* shows that the highest probability for enhancement in the MRI was found around the left inferior PV (with the UTAH method

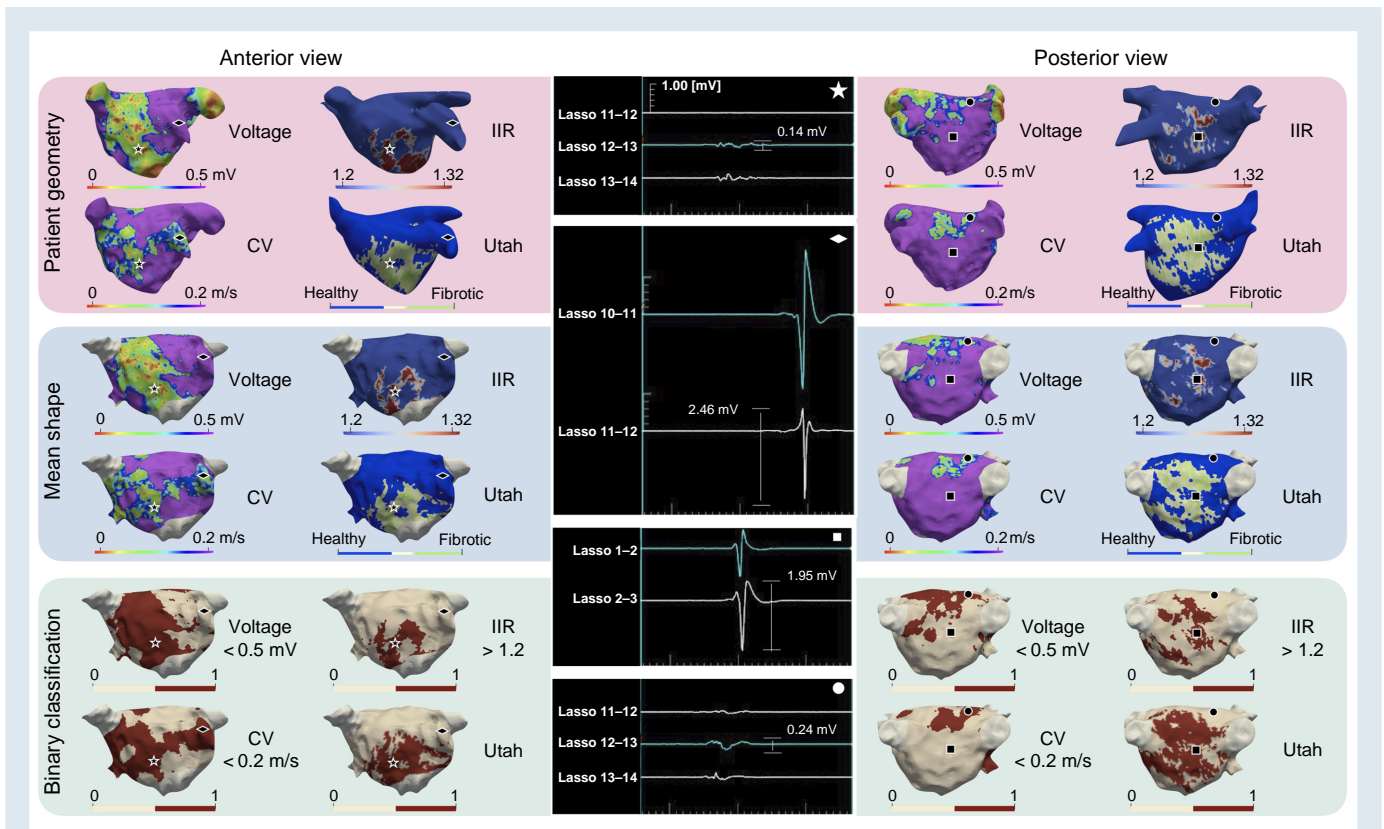
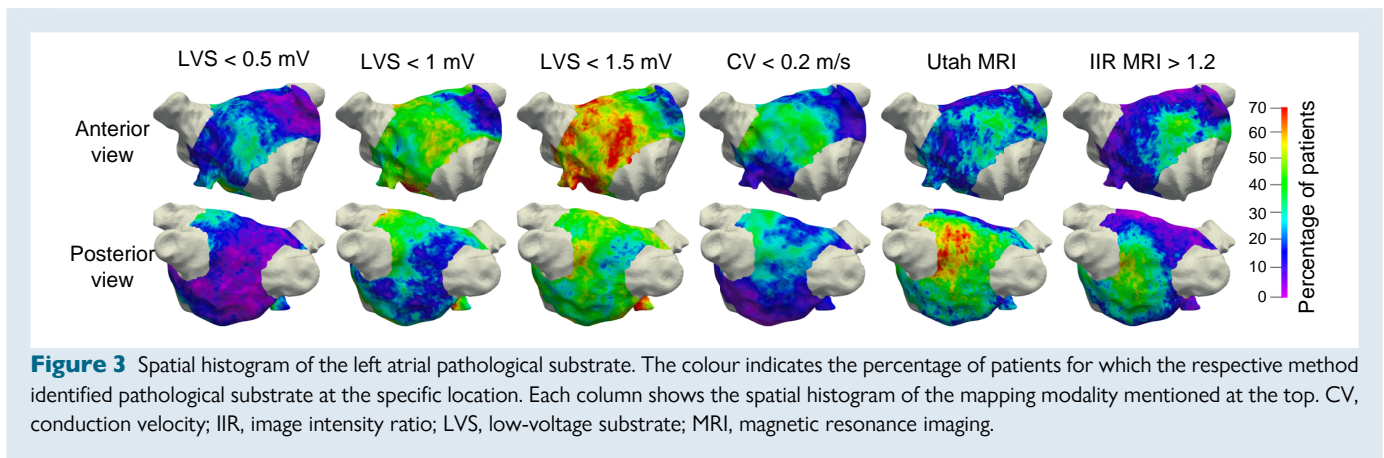
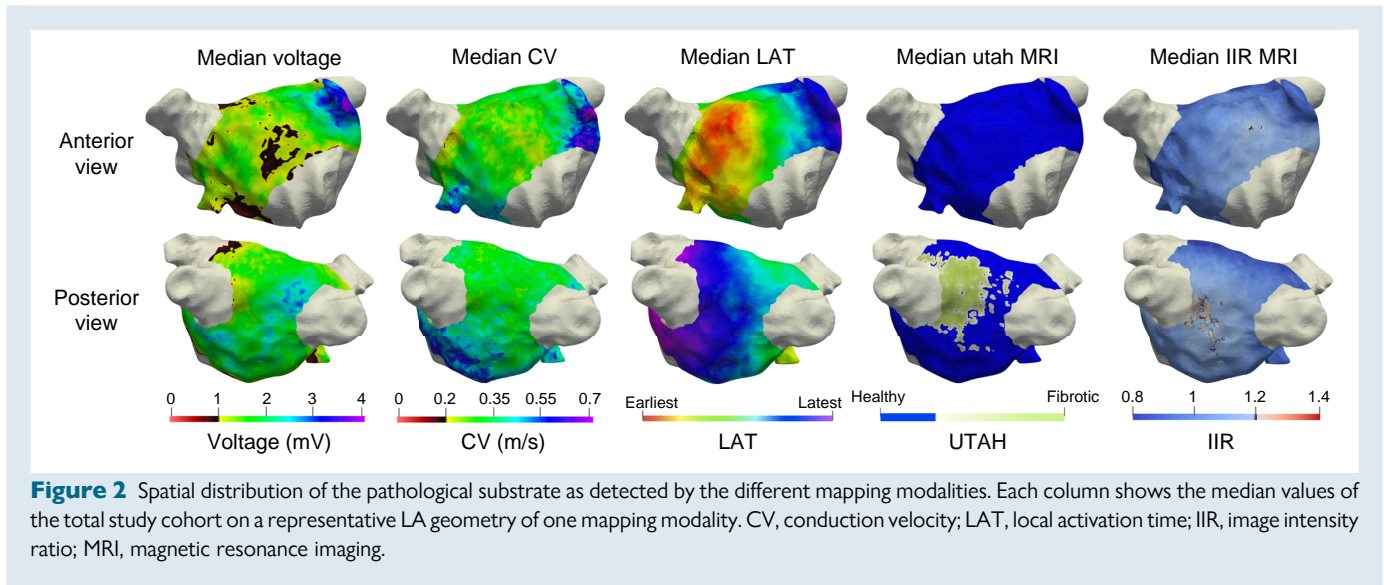


**Figure 1** Three-dimensional distribution of voltage <0.5 mV, CV <0.2 m/s, and LGE areas detected with IIR 1.2–1.32 and the UTAH method in a representative patient. The top and middle rows show the EAM and LGE-MRI information on the patient's geometry and the mean shape, respectively. The bottom row shows a binary classification, where the pathological substrate is shown in red and healthy tissue in cream. Each geometric shape (circle, square, diamond, star) represents a point on the map where the corresponding electrogram is shown in the middle column. CV, conduction velocity; IIR, image intensity ratio.



indicating ACM in 56% and IIR >1.20 in 44% of the patients). In contrast, the LVS <0.5 mV spatial histogram rarely indicated pathological substrate on the posterior wall (8% of patients). Evaluating LVS <1 mV and CV <0.2 mV, the percentage of patients with a pathological substrate for both methods was 28% in the vicinity of the left inferior PV. All methods identified a similar percentage of patients with the pathological substrate on the anterior wall (22% LVS <0.5 mV, 22% IIR >1.2, 25% UTAH, 31% CV <0.2 m/s, 42% LVS <1 mV). Activation slowing to CV <0.2 m/s mostly colocalized with LVS <0.5–1 mV.

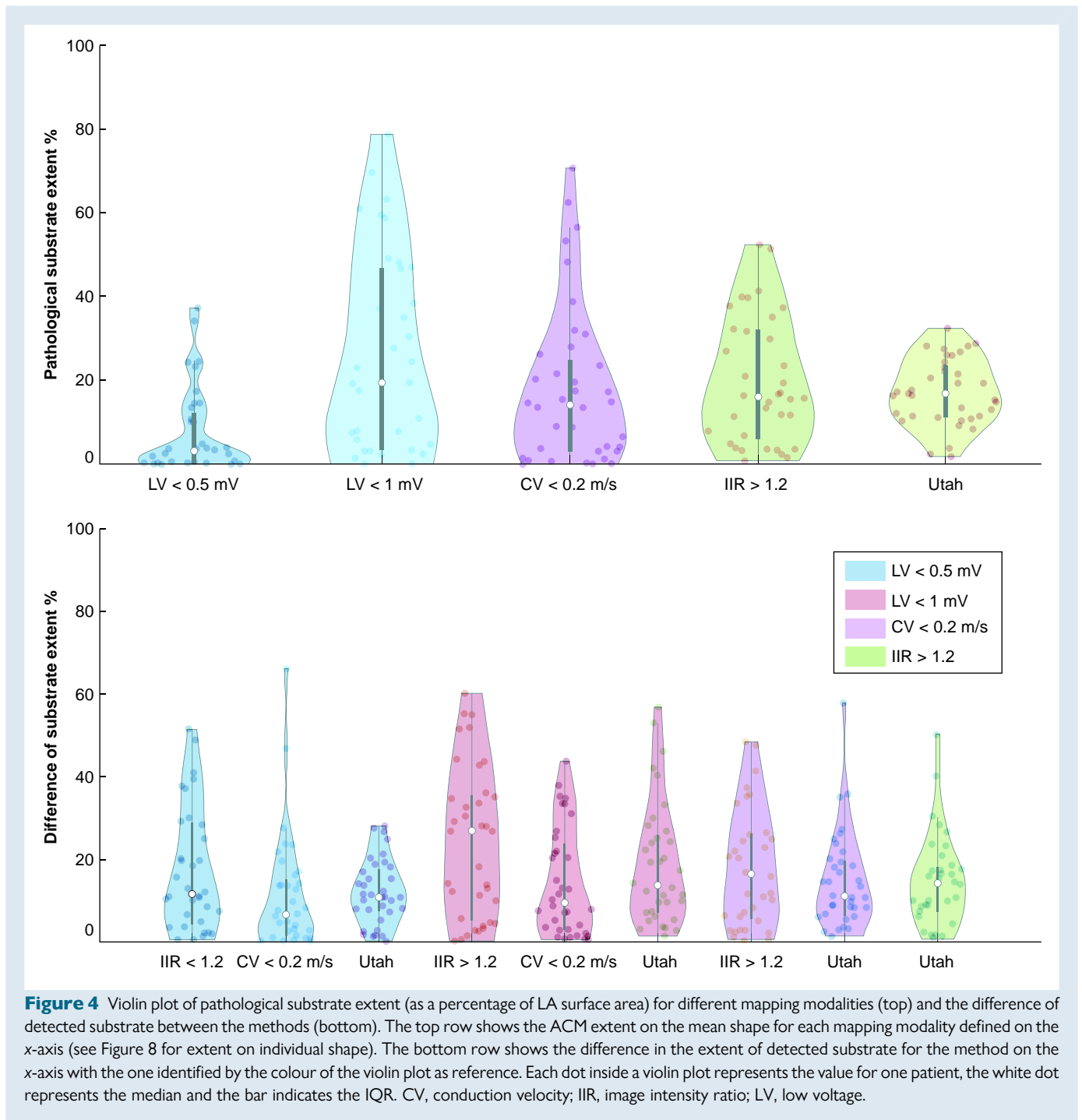
## Quantification of left atrial pathological substrate

Figure 4 reveals that the lowest difference in terms of global pathological LA substrate extent for LVS <0.5 mV and CV <0.2 m/s (median difference 6%) and LGE extent assessed with IIR >1.2 and UTAH (11%). When comparing LVS <0.5 mV and the LGE extent with the UTAH method, the difference of globally detected substrate was relatively low (median difference 10% of the LA surface; range 0–25%). While both methods detected a similar total extent of pathological LA substrate, the location of the detected substrate differed markedly between the methods (see [Supplementary material online, Figure S3](#)).

## Optimizing the late gadolinium enhancement magnetic resonance imaging threshold to identify low-voltage substrate

The 'optimized image intensity threshold' (OIIT) with respect to each patient's LA mean blood pool intensity value is shown in [Figure 5](#). For the entire LA, anterior wall and posterior wall, a linear relationship (EOIIT) was best described as  $y = 0.97x + 86$ ,  $y = 0.96x + 72$ , and  $y = 0.93x + 85$ , respectively. Here,  $x$  is the individual patient's mean blood pool intensity and  $y$  is the optimized image intensity threshold maximizing the concordance between LGE extent and LVS extent <0.5 mV ([Figure 6C](#) and [D](#)).

[Supplementary material online, Figure S4](#) demonstrates the distribution extent of LVS and LGE areas (for the entire LA, anterior and posterior LA) for both the IIR >1.2 and the new EOIIT method for all patients. Analysis of EOIIT-based LGE extent revealed similarities with LVS extent ([Figure 6A](#) and [B](#)) with good correlation on the anterior wall ( $r = 0.68$ , [Figure 6C](#)). [Supplementary material online, Section S2.4](#) provides more information on the performance of the new EOIIT compared with voltage on the posterior wall, the entire atrium, and CV mapping. Detection of LA LGE areas using the new EOIIT method still did not provide an exact match to LVS extent in every patient. This is due to the OIIT value of each patient not lying precisely on the EOIIT line ([Figure 5](#)). As seen in [Figure 6D](#), EOIIT-based LGE extent (42%) is similar to LVS extent <0.5 mV (55%) in patient 35. However, the locations of detected substrate remain different between voltage mapping and LGE-MRI.



**Figure 4** Violin plot of pathological substrate extent (as a percentage of LA surface area) for different mapping modalities (top) and the difference of detected substrate between the methods (bottom). The top row shows the ACM extent on the mean shape for each mapping modality defined on the x-axis (see Figure 8 for extent on individual shape). The bottom row shows the difference in the extent of detected substrate for the method on the x-axis with the one identified by the colour of the violin plot as reference. Each dot inside a violin plot represents the value for one patient, the white dot represents the median and the bar indicates the IQR. CV, conduction velocity; IIR, image intensity ratio; LV, low voltage.

## Estimated optimized image intensity threshold enables late gadolinium enhancement magnetic resonance imaging-based diagnosis of patients with atrial cardiomyopathy presenting low-voltage substrate

Despite the discrepancies in exact quantitative and spatial match between EOIT-based LGE extent and LVS extent, we hypothesized that the new EOIT method could be useful to diagnose patients with

significant ACM. Diagnosis of clinically relevant ACM was based on presence of LVS <0.5 mV at >5% of LA surface area, which was previously shown to be predictive for arrhythmia recurrences in persistent AF patients undergoing a PVI-only approach.<sup>10,27,28</sup> Receiver operating characteristic (ROC) analysis determined the best quantitative LGE extent for ACM diagnosis (Figure 7A–C). Atrial cardiomyopathy diagnosis was most accurate when using the EOIT-based LGE extent >5% at the anterior LA [sensitivity: 83%, specificity: 79%, area under the curve (AUC): 0.89] in contrast to >12% LGE extent for IIR >1.20 (sensitivity: 75%, specificity: 62%, AUC: 0.67). Figure 8 additionally illustrates these results, where the dashed lines correspond to the identified optimal

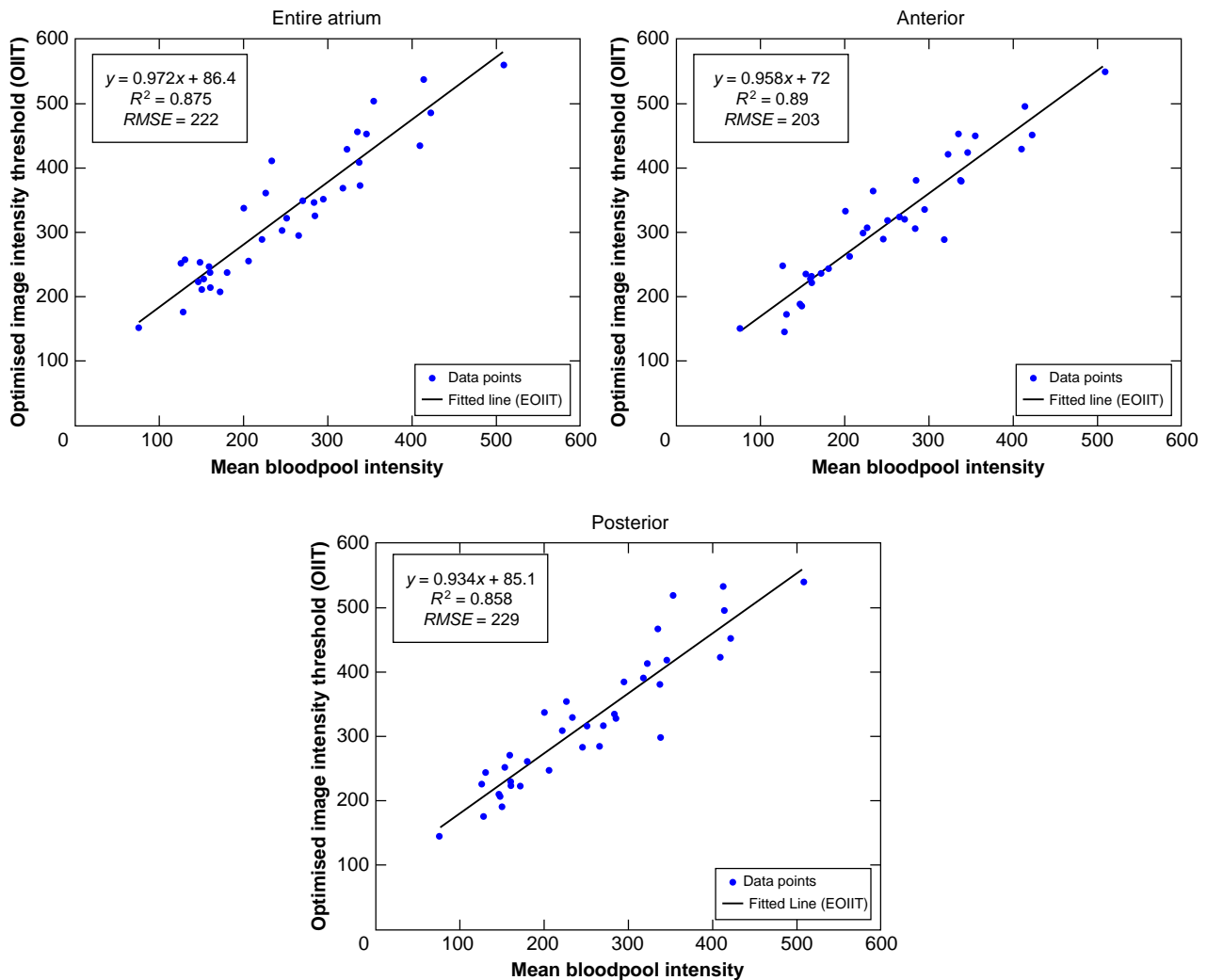


**Figure 5** Identification of the EOIIT using linear correlation between the individual patient's mean blood pool intensity (x-axis) and optimal image intensity threshold (y-axis). From left to right, the results for the entire LA, anterior wall, and posterior wall are shown. Each dot represents one patient and the line is the best linear fit. EOIIT, estimated optimized image intensity threshold; OIIT, optimized image intensity threshold.

thresholds. For the entire LA, the EOIIT-based (>4%) and UTAH-based (>15%) LGE extent had a sensitivity and specificity of 67 and 79% (AUC: 0.69) and 100 and 71% (AUC: 0.81), respectively.

Low-voltage substrate <0.5 mV at  $\geq 5\%$  of the total LA surface was predictive of AF recurrence (58.3 vs. 29.2%,  $P = 0.047$ , Figure 7D). The optimal cut-off values identified above were also predictive for EOIIT-based LGE extent >5% at the anterior LA (60.0 vs. 23.8%,  $P = 0.033$ , Figure 7E) but not statistically significant for IIR >1.2 (50.0 vs. 27.8%,  $P = 0.14$ , Figure 7F). Conduction velocity <0.2 m/s at 5% of the total LA surface was predictive as well (52.2 vs. 15.4%,  $P = 0.036$ , Figure 7G).

## Discussion

### Main findings

This study investigated the discrepancies of different mapping modalities for detecting LA pathological fibrotic substrate. Four key findings can be reported:

- (1) Important discordances exist in the extent and spatial localization of identified pathological left atrial substrate when comparing electro-

anatomical voltage and CV mapping to LGE-MRI. These discordances exist with all LGE detection protocols and all three bipolar voltage thresholds (<0.5, <1.0, and <1.5 mV). The observed substrate differences between LGE-MRI and EAM are more pronounced on the posterior LA wall.

- (2) The extent of LA slow conduction areas (CV <0.2 m/s) correlate moderately ( $r = 0.57$ ) with LVS (<0.5 mV).
- (3) Applying the new EOIIT method on the anterior LA wall enables LGE-MRI-based diagnosis of AF patients with ACM (presenting significant LVS <0.5 mV at  $\geq 5\%$  total LA surface) with a sensitivity of 83% and a specificity of 79%.
- (4) The new EOIIT method is predictive of arrhythmia recurrence ( $P = 0.033$ ).

### Clinical significance of left atrial cardiomyopathy in patients with atrial fibrillation

Several studies have demonstrated the relevance of LA-LVS <0.5 mV regarding increased arrhythmia recurrences within 12 months

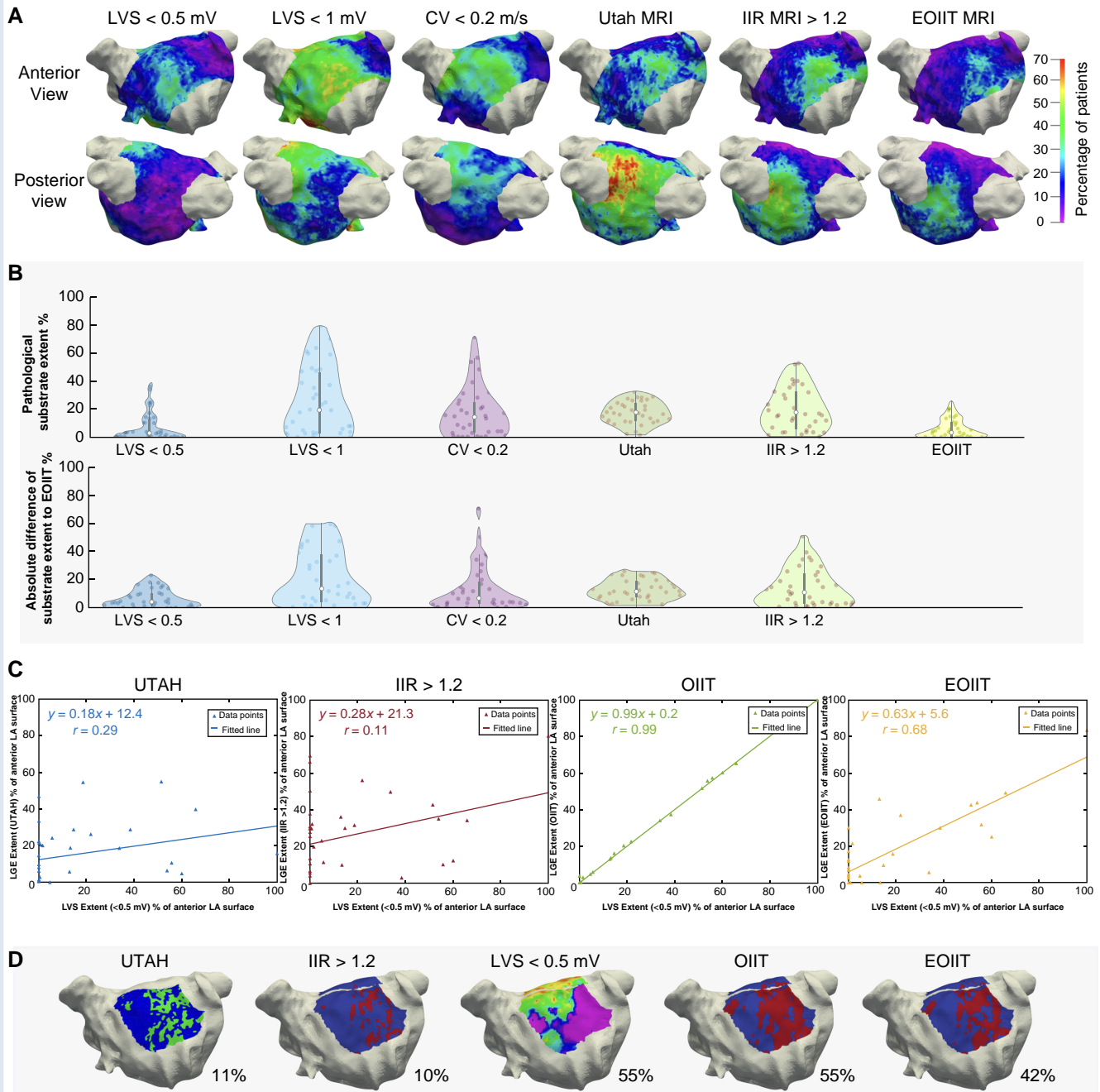


**Figure 6** Estimated optimized image intensity threshold. (A) Spatial histogram of each mapping modality including the new EOIIT method. (B) Violin plot showing the pathological substrate extent on the mean shape for different mapping modalities and the difference between them and the new EOIIT method. (C) Percentage of substrate extent of each LGE-MRI method vs. LVS extent for the anterior LA wall. Note that OIIT analysis can only be performed when both LGE-MRI and EAM are available in a patient and thus does not add clinical value to pure LGE-MRI. (D) Distribution extent of LVS and LGE areas for the anterior LA in patient 35. CV, conduction velocity; EOIIT, estimated optimized image intensity threshold; IIR, image intensity ratio; LVS, low-voltage substrate; MRI, magnetic resonance imaging; OIIT, optimized image intensity threshold.

following PVI for AF.<sup>21,29</sup> Since the correlation of bipolar electrogram voltage with the amount of viable tissue in histology has been shown<sup>30</sup> and ablation of LVS improves arrhythmia freedom,<sup>10</sup> this modality was used as a reference.

Recently, the predictive value of LVS <0.5 mV at >5% of LA surface was demonstrated concerning arrhythmia recurrence rate following PVI.<sup>27</sup> Therefore, this LVS extent was used as a cut-off in the current study. In addition, the presence of ACM, as assessed by LA-LVS is



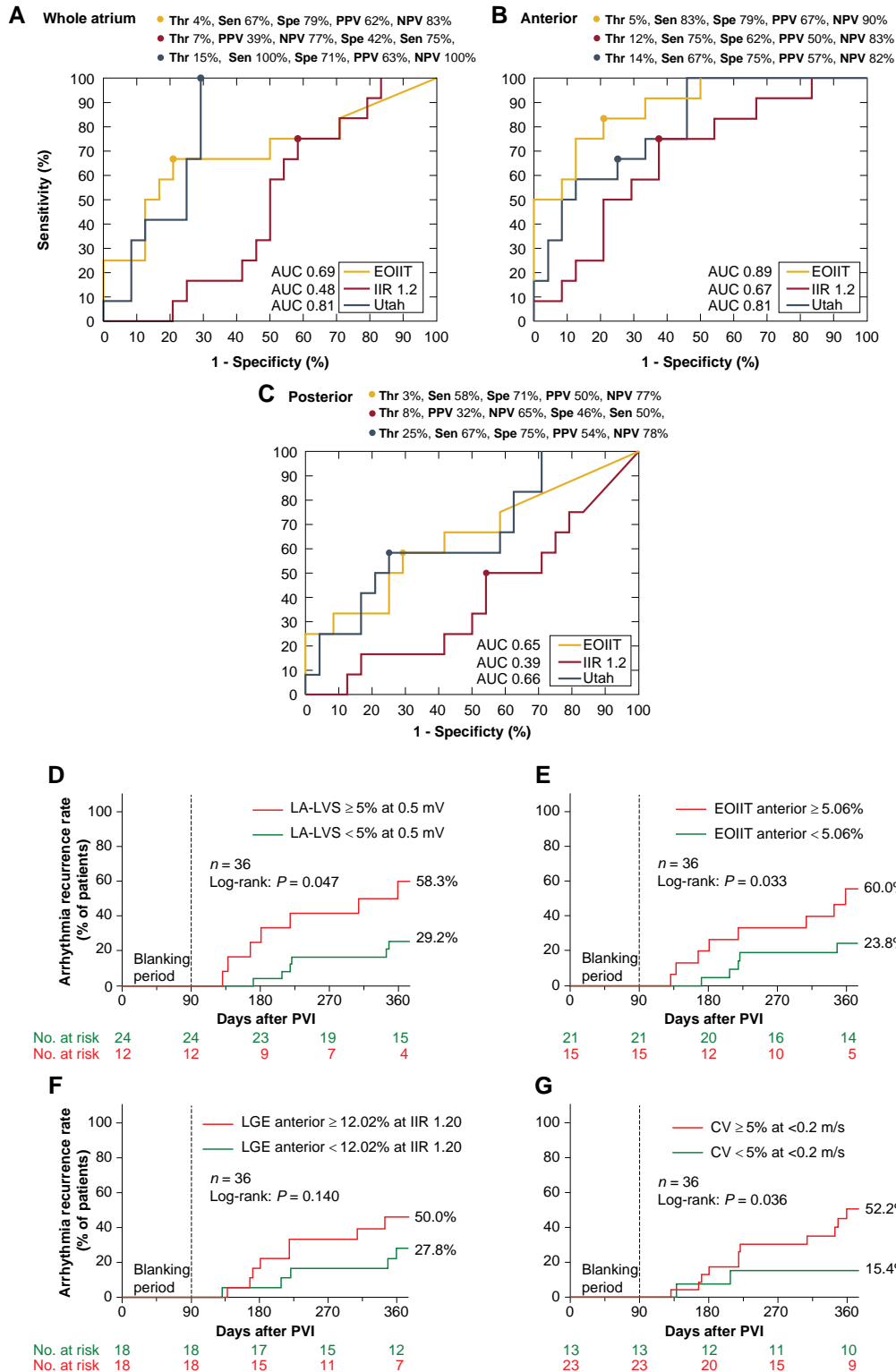
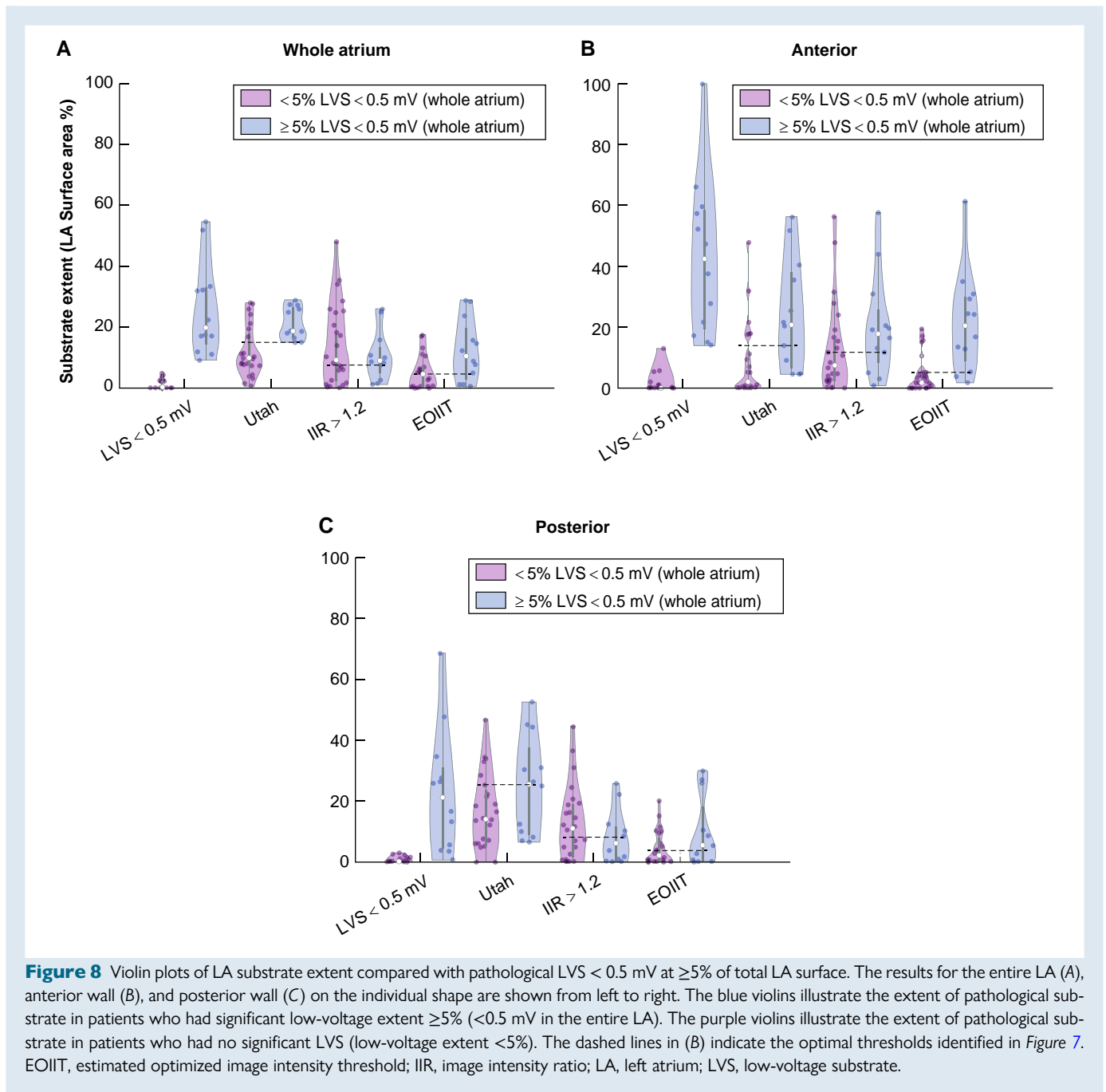


**Figure 7** Receiver operating characteristic analysis determines the diagnostic LGE extent that identifies patients with ACM (defined as LVS  $< 0.5$  mV at  $\geq 5\%$  of total LA surface). (A) using LGE extent from the entire LA, (B) from the anterior, and (C) from the posterior wall only. Yellow and red lines show the ROC of the EOIIT-based and IIR  $> 1.2$  based methods for LGE-based ACM detection, respectively. Kaplan–Meier curves for prediction of arrhythmia recurrence using different metrics and their respective cut-off values: (D) LVS  $< 0.5$  mV at  $\geq 5\%$  of total LA surface, (E) LGE  $>$  EOIIT at  $\geq 5\%$  of the anterior wall, (F) IIR  $> 1.2$  at  $\geq 12\%$  of the anterior wall, (G) CV  $< 0.2$  m/s at  $\geq 5\%$  of the total LA surface. AUC, area under the curve; LGE, late gadolinium enhancement; PVI, pulmonary vein isolation.



associated with an increased risk for ischaemic stroke.<sup>31</sup> Therefore, the most recent European guidelines on the management of patients with AF recommend a diagnosis of ACM in order to initiate therapeutic efforts in limiting progression and related complications of ACM.<sup>1</sup>

### Regional differences in detected left atrial substrate—comparing electro-anatomical mapping to late gadolinium enhancement magnetic resonance imaging

Pathological substrate was most consistently found with all modalities (low voltage, slow conduction, and LGE-MRI) at the anterior LA wall (20–40% of patients), confirming preferential fibrotic remodelling in

this area. Across the whole LA, the CV was  $0.48 \pm 0.39$  m/s, which is comparable to previous findings in AF patients.<sup>11,12</sup> During open heart epicardial mapping combined with discrete velocity vectors, van Schie *et al.*<sup>32</sup> reported 0.89 m/s in the left atrium of 58 paroxysmal AF patients. Our study confirms that low-voltage and slow-conduction areas most frequently develop on the anteroseptal LA wall and the roof.<sup>28,33</sup>

In contrast, both the UTAH and IIR >1.20 methods most frequently detected LGE at the left posterior LA adjacent to the descending aorta (56 and 44%, respectively), which is consistent with previous reports.<sup>18,26,34</sup> Caixal *et al.*<sup>34</sup> demonstrated that the spatial proximity of the posterior LA wall to the descending aorta can determine the degree of LGE in this region. Caixal *et al.* and Spragg *et al.* reported a reduction of bipolar voltages and agreement between LGE-MRI and low-voltage regions at the left posterior LA.<sup>35,36</sup> However, these were relatively

small patient cohorts (16 and 10 patients with only three persistent AF patients in both studies). The current study, which includes 36 persistent AF patients and applies an extended approach to study the spatial extent and distribution between the methods, found that CV  $<0.2$  m/s was observed in only 28% and LVS  $<0.5$  mV in 8% of patients on the posterior wall. Although voltage reduction can be observed in some patients within this LA area, the electrograms are non-fractionated and display voltages  $>1.0$  mV in  $>70\%$  of patients. Thus, discrepancies in substrate qualification remain, even when defining LVS as  $<1.0$  or  $<1.5$  mV (Figure 3).

## Differences in substrate assessment methods

Pathological substrate is frequently found in opposite locations when comparing electrophysiological substrate to LGE areas. When considering all patients (see [Supplementary material online, Figures S3 and S4](#)), the distribution and location of the pathological substrates are well correlated in some, while they differ in other patients. This discrepancy in substrate localization (despite rather high global substrate extent match) may contribute to the difficulties in achieving satisfactory long-term success in prospective studies based on substrate ablation in persistent AF patients.<sup>3,5–7</sup> Azzolin *et al.*<sup>37</sup> highlighted the importance of accurate substrate identification in a well-controlled computational ablation study comparing different substrate assessment modalities and different ablation strategies using the same cohort as in the present study. The discrepancy in LGE-MRI vs. LVS assessment led to 35–41% lower *in silico* AF termination rates. Additionally, the specific type of fibrotic tissue represented in the model affects AF dynamics.<sup>38</sup>

One could hypothesize that the mapping modalities provide complementary information that could be leveraged when determining ablation targets. It has been reported that different fibrotic patterns of various types and densities exist, which could affect the mapping modalities differently.<sup>39</sup> Small patchy fibrotic strands with small contributions to the electrogram signal may be compensated by surrounding myocytes and atrial far-fields, causing ‘undersensing’ of fibrotic areas. Another aspect is the proximity of the descending aorta to the LA posterior wall. Caixal *et al.*<sup>34</sup> found more LGE in areas closer to the descending aorta. While also voltage and CV were lower in these areas in a bimodally mapped subcohort of 16 patients, partial volume effects in the thin posterior wall<sup>40</sup> may also play a role. Another factor potentially contributing to the differences in substrate assessment methods is that fatty tissue infiltration might not be identifiable by LGE-MRI but affect LVS and arrhythmia propensity.<sup>41</sup> However, endocardial voltage measurements are dominated by the first 1–2 mm of endocardial tissue while fatty infiltrations are often concentrated on the epicardial surface. In contrast, fibrosis solely expressed on the epicardial side may be hidden by endocardial catheters. Zahid *et al.*<sup>14</sup> reported reduction in left atrial CV in hypertrophic cardiomyopathy patients despite normal bipolar voltage. Using intra-operative epicardial mapping, van Schie *et al.*<sup>42</sup> analysed local directional heterogeneity and conduction. Compared with SR, premature atrial contractions led to increased local directional heterogeneity particularly around the PVs and in Bachmann’s bundle.

In contrast to a previous analysis of this cohort on a global level,<sup>19</sup> we performed a point-by-point analysis in this work. Examining all three methods (CV, LVS, and LGE-MRI) may help to comprehensively assess the pathological LA substrate with a more localized analysis than possible with the ECG.<sup>43,44</sup> In particular, big data analyses using machine learning approaches can be promising when high-quality data of sufficient size are available. However, the fact that ablation of LVS improved SR maintenance rate in the ERASE-AF RCT<sup>10</sup> while ablation of LGE areas in the DECAAF II RCT<sup>5</sup> did not challenge the notion of a major arrhythmogenic role of LGE areas detected using the UTAH method for human AF.

## Optimizing late gadolinium enhancement magnetic resonance imaging thresholds

Identifying the same regions of pathological substrate across all established mapping modalities was not possible with the current techniques. Therefore, we sought to improve LGE-based detection of total LA-LVS extent, thus allowing a more accurate ACM diagnosis. In this analysis, new LGE-MRI thresholds were identified, which, similarly to the IIR method, can be determined using each patient’s mean blood pool intensity.

Benito *et al.*<sup>17</sup> studied 30 patients with various stages of AF. They set the threshold to determine pathological substrate at  $>1.20$ . As discussed, determining the exact extent of pathological substrate on the thin posterior wall remains challenging, which may be related to MRI resolution.<sup>45</sup> Since the high-intensity areas were mostly located on the posterior wall across the patient cohort, taking the mean tissue IIR + 2 standard deviations as the threshold in the study by Benito *et al.* was potentially influenced by these high-intensity areas on the posterior wall. Therefore, their suggested threshold might be too high to identify pathological substrate on the anterior wall.

The new EOIT-based thresholds presented in this work, however, can provide a better estimate of the LVS extent located on the anterior LA-wall, thus enabling the diagnosis of ACM in individuals. The proximity of the optimal EOIT-based anterior LA surface extent cut-off of 5.06% to the LA-LVS extent  $\geq 5\%$  provides a proof of the EOIT concept. Previous studies revealed that LVS first develops on the anterior LA, and in later stages involves the posterior LA wall.<sup>28,33</sup> Therefore, diagnosis of ACM that is based on analysis of LGE presence on the anterior LA wall is both sensitive and specific for ACM diagnosis, as shown in our study. Accurate diagnosis of ACM provides a deeper insight into whether a PVI-only treatment would be sufficient or if additional LA mapping and ablation is needed as demonstrated by the higher arrhythmia recurrence in patients with  $>5\%$  EOIT-based substrate on the anterior wall (60.0 vs. 23.8%,  $P = 0.033$ ).

## Limitations

The cohort size for this study was relatively small. Thus, overfitting may play a role when computing the linear fit to determine the new LGE-MRI thresholds. To ameliorate this effect, leave-one-out-cross validation was used. In the future, larger cohorts would be desirable which allow for subgroup analyses per gender or age. The results obtained here may also be specific to the distribution of substrate in our cohort. The new EOIT LGE-MRI-based ACM diagnosis needs further validation in larger external cohorts. Furthermore, adaptations for determination of lab-specific EOIT curves may be necessary due to the fact that LGE detection depends on multiple factors (e.g. type, dosage, and timing of contrast injection, magnetic field strength, acquisition protocol). We used blood pool normalization to mitigate the effects of individual characteristics such as body mass index, haematocrit, and renal function, which have an impact on gadolinium wash-in and wash-out.

In addition to the three modalities assessed in this study, others as for example left atrial wall thickness and lipomatous tissue may yield valuable complementary information<sup>46</sup> but would likely depend on additional computed tomography imaging.<sup>40</sup>

## Conclusions

Important discordances exist in localization of detected pathological LA-LVS vs. slow conduction zones vs. LGE areas in MRI. Despite a good correlation between the extent of LA-LVS and EOIT-LGE areas, the exact locations of identified pathological substrate differ. The new EOIT method increase concordance of LGE-MRI-based and LVS-based ACM diagnosis in ablation-naïve AF patients and is predictive for PVI

success. The residual discrepancy suggests that the three substrate assessment methods may provide complementary information.

## Supplementary material

Supplementary material is available at *Europace* online HCM.

### Funding

We gratefully acknowledge financial support by Deutsche Forschungsgemeinschaft (DFG) through DO637/22-3, by the Ministerium für Wissenschaft, Forschung und Kunst Baden-Württemberg through the Research Seed Capital (RiSC) program and by Medtronic. This work has received funding from the European Union's Horizon 2020 research and innovation programme under the Marie Skłodowska-Curie grant agreement No.766082. This work was supported by the EMPIR programme co-financed by the participating states and from the European Union's Horizon 2020 research and innovation programme under grant MedalCare 18HLT07.

**Conflict of interest:** We have read the journal's policy and the authors of this manuscript have the following competing interests: R.M.F.V., B.R.F., and A.V.C. are employees of Adas 3D Medical. This investigator-initiated study was financially supported by Medtronic. Medtronic had no influence on collection, analysis, and interpretation of data, in the writing of the report, and in the decision to submit the article for publication. All remaining authors declared no conflicts of interest.

### Data availability

The figures within the article and [Supplementary material online](#) show detailed analyses for all patients used. Raw patient data cannot be shared without additional IRB approval and patient consent. Requests should be directed to the IRB of Freiburg University Hospital.

### References

- Hindricks G, Potpara T, Dagres N, Arbelo E, Bax JJ, Blomström-Lundqvist C et al. 2020 ESC guidelines for the diagnosis and management of atrial fibrillation developed in collaboration with the European Association for Cardio-Thoracic Surgery (EACTS). *Eur Heart J* 2021;**42**:373–498.
- Taghji P, Haddad ME, Philips T, Wolf M, Knecht S, Vandekerckhove Y et al. Evaluation of a strategy aiming to enclose the pulmonary veins with contiguous and optimized radiofrequency lesions in paroxysmal atrial fibrillation: a pilot study. *JACC Clin Electrophysiol* 2018;**4**:99–108.
- Verma A, Jiang C-Y, Betts TR, Chen J, Deisenhofer I, Mantovan R et al. Approaches to catheter ablation for persistent atrial fibrillation. *N Engl J Med* 2015;**372**:1812–22.
- Goette A, Kalman JM, Aguinaga L, Akar J, Cabrera JA, Chen SA et al. EHRA/HRS/APHRS/SOLAECE expert consensus on atrial cardiomyopathies: definition, characterization, and clinical implication. *Heart Rhythm* 2017;**14**:e3–40.
- Marrouche NF, Wazni O, McGann C, Greene T, Dean JM, Dagher L et al. Effect of MRI-guided fibrosis ablation vs conventional catheter ablation on atrial arrhythmia recurrence in patients with persistent atrial fibrillation: the DECAAF II randomized clinical trial. *JAMA* 2022;**327**:2296–305.
- Yang B, Jiang C, Lin Y, Yang G, Chu H, Cai H et al. STABLE-SR (electrophysiological substrate ablation in the left atrium during sinus rhythm) for the treatment of nonparoxysmal atrial fibrillation. *Circ Arrhythm Electrophysiol* 2017;**10**:e005405.
- Bisbal F, Benito E, Teis A, Alarcón F, Sarrias A, Caixal G et al. Magnetic resonance imaging-guided fibrosis ablation for the treatment of atrial fibrillation. *Circ Arrhythm Electrophysiol* 2020;**13**:e008707.
- Jadidi A, Nothstein M, Chen J, Lehmann H, Dössel O, Allgeier J et al. Specific electrogram characteristics identify the extra-pulmonary vein arrhythmogenic sources of persistent atrial fibrillation—characterization of the arrhythmogenic electrogram patterns during atrial fibrillation and sinus rhythm. *Sci Rep* 2020;**10**:9147.
- Seitz J, Bars C, Théodore G, Beurtheret S, Lellouche N, Bremond M et al. AF ablation guided by spatiotemporal electrogram dispersion without pulmonary vein isolation: a wholly patient-tailored approach. *J Am Coll Cardiol* 2017;**69**:303–21.
- Huo Y, Gaspar T, Schönbauer R, Wójcik M, Fiedler L, Roithinger FX et al. Low-voltage myocardium-guided ablation trial of persistent atrial fibrillation. *NEJM Evid* 2022;**1**:EVID0a2200141.
- Zheng Y, Xia Y, Carlson J, Kongstad O, Yuan S. Atrial average conduction velocity in patients with and without paroxysmal atrial fibrillation. *Clin Physiol Funct Imaging* 2016;**37**:596–601.
- Verma B, Oesterlein T, Loewe A, Luik A, Schmitt C, Dössel O. Regional conduction velocity calculation from clinical multichannel electrograms in human atria. *Comput Biol Med* 2018;**92**:188–96.
- Ohguchi S, Inden Y, Yanagisawa S, Fujita R, Yasuda K, Katagiri K et al. Regional left atrial conduction velocity in the anterior wall is associated with clinical recurrence of atrial fibrillation after catheter ablation: efficacy in combination with the ipsilateral low voltage area. *BMC Cardiovasc Dis* 2022;**22**:457.
- Zahid S, Malik T, Peterson C, Tarabnis C, Dai M, Katz M et al. Conduction velocity is reduced in the posterior wall of hypertrophic cardiomyopathy patients with normal bipolar voltage undergoing ablation for paroxysmal atrial fibrillation. *J Interv Card Electrophysiol* 2023. Epub ahead of print.
- Oakes RS, Badger TJ, Kholmovski EG, Akoum N, Burgon NS, Fish EN et al. Detection and quantification of left atrial structural remodeling with delayed-enhancement magnetic resonance imaging in patients with atrial fibrillation. *Circulation* 2009;**119**:1758–67.
- Marrouche NF, Wilber D, Hindricks G, Jais P, Akoum N, Marchlinski F et al. Association of atrial tissue fibrosis identified by delayed enhancement MRI and atrial fibrillation catheter ablation: the DECAAF study. *J Am Med Assoc* 2014;**311**:498–506.
- Benito EM, Carlosena-Remirez A, Guasch E, Prat-González S, Perea RJ, Figueras R et al. Left atrial fibrosis quantification by late gadolinium-enhanced magnetic resonance: a new method to standardize the thresholds for reproducibility. *Europace* 2017;**19**:1272–9.
- Chen J, Arentz T, Cochet H, Müller-Edenborn B, Kim S, Moreno-Weidmann Z et al. Extent and spatial distribution of left atrial arrhythmogenic sites, late gadolinium enhancement at magnetic resonance imaging, and low-voltage areas in patients with persistent atrial fibrillation: comparison of imaging vs. electrical parameters of fibrosis and arrhythmogenesis. *Europace* 2019;**21**:1484–93.
- Eichenlaub M, Mueller-Edenborn B, Minners J, Figueras i Ventura RM, Forcada BR, Colomer AV et al. Comparison of various late gadolinium enhancement magnetic resonance imaging methods with high-definition voltage and activation mapping for detection of atrial cardiomyopathy. *Europace* 2022;**24**:1102–11.
- Boyle PM, Sarairah S, Kwan KT, Scott GD, Mohamedali F, Anderson CA et al. Elevated fibrosis burden as assessed by MRI predicts cryoballoon ablation failure. *J Cardiovasc Electrophysiol* 2023;**34**:302–12.
- Jadidi AS, Lehmann H, Keyl C, Sorrel J, Markstein V, Minners J et al. Ablation of persistent atrial fibrillation targeting low-voltage areas with selective activation characteristics. *Circ Arrhythm Electrophysiol* 2016;**9**:e002962.
- Nairn D, Lehmann H, Müller-Edenborn B, Schuler S, Arentz T, Dössel O et al. Comparison of unipolar and bipolar voltage mapping for localization of left atrial arrhythmogenic substrate in patients with atrial fibrillation. *Front Physiol* 2020;**11**:575846.
- Anderson KP, Walker R, Urie P, Ershler PR, Lux RL, Karwande SV. Myocardial electrical propagation in patients with idiopathic dilated cardiomyopathy. *J Clin Invest* 1993;**92**:122–40.
- D. Nairn, C. Nagel, B. Müller-Edenborn, H. Lehmann, T. Arentz, O. Dössel et al. Optimal regional voltage thresholds for identifying ablation targets in patients with atrial fibrillation. *Comput Cardiol Conference (CinC)* 2021;**48**:1–4.
- Nagel C, Schuler S, Dössel O, Loewe A. A bi-atrial statistical shape model for large-scale in silico studies of human atria: model development and application to ECG simulations. *Med Image Anal* 2021;**74**:102210.
- Higuchi K, Cates J, Gardner G, Morris A, Burgon NS, Akoum N et al. The spatial distribution of late gadolinium enhancement of left atrial magnetic resonance imaging in patients with atrial fibrillation. *JACC Clin Electrophysiol* 2018;**4**:49–58.
- Müller-Edenborn B, Moreno-Weidmann Z, Venier S, Defaye P, Park C, Guerra J et al. Determinants of fibrotic atrial cardiomyopathy in atrial fibrillation: a multicenter observational study of the RETAC (reseau européen de traitement d'arrhythmies cardiaques)-group. *Clin Res Cardiol* 2021;**111**:1018–27.
- Müller-Edenborn B, Chen J, Allgeier J, Didenko M, Moreno-Weidmann Z, Neumann FJ et al. Amplified sinus-P-wave reveals localization and extent of left atrial low-voltage substrate: implications for arrhythmia freedom following pulmonary vein isolation. *Europace* 2019;**22**:240–9.
- Rolf S, Kircher S, Arya A, Eitel C, Sommer P, Richter S et al. Tailored atrial substrate modification based on low-voltage areas in catheter ablation of atrial fibrillation. *Circ Arrhythm Electrophysiol* 2014;**7**:825–33.
- Glashan CA, Tofig BJ, Beukers H, Tao Q, Blom SA, Villadsen PR et al. Multielectrode unipolar voltage mapping and electrogram morphology to identify post-infarct scar geometry: validation by histology. *JACC Clin Electrophysiol* 2022;**8**:437–49.
- Müller P, Makimoto H, Dietrich JW, Fochler F, Nentwich K, Krug J et al. Association of left atrial low-voltage area and thromboembolic risk in patients with atrial fibrillation. *Europace* 2018;**20**:359–65.
- van Schie MS, Heida A, Taverne YJH, Bogers AJC, de Groot NMS. Identification of local atrial conduction heterogeneities using high-density conduction velocity estimation. *Europace* 2021;**23**:1815–25.
- Huo Y, Gaspar T, Pohl M, Sitzy J, Richter U, Neudeck S et al. Prevalence and predictors of low voltage zones in the left atrium in patients with atrial fibrillation. *Europace* 2018;**20**:956–62.

34. Caixal G, Althoff T, Garre P, Alarcón F, NuñezGarcía M, Benito EM et al. Proximity to the descending aorta predicts regional fibrosis in the adjacent left atrial wall: aetiopathogenic and prognostic implications. *Europace* 2021;**23**:1559–67.
35. Spragg DD, Khurram I, Zimmerman SL, Yarmohammadi H, Barcelon B, Needleman M et al. Initial experience with magnetic resonance imaging of atrial scar and co-registration with electroanatomic voltage mapping during atrial fibrillation: success and limitations. *Heart Rhythm* 2012;**9**:2003–9.
36. Caixal G, Alarcón F, Althoff TF, Nuñez-García M, Benito EM, Borràs R et al. Accuracy of left atrial fibrosis detection with cardiac magnetic resonance: correlation of late gadolinium enhancement with endocardial voltage and conduction velocity. *Europace* 2020;**23**:380–8.
37. Azzolin L, Eichenlaub M, Nagel C, Nairn D, Sanchez J, Unger L et al. Personalized ablation vs. conventional ablation strategies to terminate atrial fibrillation and prevent recurrence. *Europace* 2022;**25**:211–22.
38. Roney CH, Bayer JD, Zahid S, Meo M, Boyle PMJ, Trayanova NA et al. Modelling methodology of atrial fibrosis affects rotor dynamics and electrograms. *Europace* 2016;**18**:iv146–55.
39. Hansen BJ, Zhao J, Fedorov VV. Fibrosis and atrial fibrillation: computerized and optical mapping: a view into the human atria at submillimeter resolution. *JACC Clin Electrophysiol* 2017;**3**:531–46.
40. Whitaker J, Rajani R, Chubb H, Gabrawi M, Varela M, Wright M et al. The role of myocardial wall thickness in atrial arrhythmogenesis. *Europace* 2016;**18**:1758–72.
41. Canpolat U, Aytemir K, Yorgun H, Asil S, Dural M, Özer N. The impact of echocardiographic epicardial fat thickness on outcomes of cryoballoon-based atrial fibrillation ablation. *Echocardiography* 2016;**33**:821–9.
42. van Schie MS, Misier NLR, Ebrahimi PR, Heida A, Kharbanda RK, Taverne YJHJ et al. Premature atrial contractions promote local directional heterogeneities in conduction velocity vectors. *Europace* 2023;**25**:1162–71.
43. Nagel C, Luongo G, Azzolin L, Schuler S, Dössel O, Loewe A. Non-invasive and quantitative estimation of left atrial fibrosis based on p waves of the 12-lead ECG—a large-scale computational study covering anatomical variability. *J Clin Med* 2021;**10**:1797.
44. Luongo G, Azzolin L, Schuler S, Rivolta MW, Almeida TP, Martínez JP et al. Machine learning enables noninvasive prediction of atrial fibrillation driver location and acute pulmonary vein ablation success using the 12-lead ECG. *Cardiovasc Digit Health J* 2021;**2**:126–36.
45. Ho SY, Cabrera JA, Sanchez-Quintana D. Left atrial anatomy revisited. *Circ Arrhythm Electrophysiol* 2012;**5**:220–8.
46. Falasconi G, Penela D, Soto-Iglesias D, Francia P, Teres C, Saglietto A et al. Personalized pulmonary vein antrum isolation guided by left atrial wall thickness for persistent atrial fibrillation. *Europace* 2023;**25**:euaad118.